Paper 91

Proceedings of the Eleventh International Conference
on Computational Structures Technology,
B.H.V. Topping, (Editor),
Civil-Comp Press, Stirlingshire, Scotland

A Comprehensive Dynamic Model for Axial, Flexural and Torsional Vibration of a CANDU Fuel Element

S.D. Yu and M. Fadaee
Department of Mechanical and Industrial Engineering
Ryerson University, Toronto, Ontario, Canada

Abstract

This paper presents a comprehensive dynamic model based on a mixed beam finite element scheme for free axial, flexural and torsional vibration of a CANDU fuel element Numerical results obtained for an outer fuel element consisting of fuel sheath with and without bearing pads as appendages show that the effects of the appendages on the natural frequencies and mode shapes are significant. In developing a computational model for a fuel bundle or a string of fuel bundles for fretting and wear analysis, it is important to consider the effects of appendages.

Keywords: axial vibration, CANDU fuel element, flexural vibration, torsional vibration.

1 Introduction

In a typical CANDU reactor fuel channel, there are a string of 12 fuel bundles lined up axially and placed inside a pressure tube in a horizontal manner, as illustrated in Figure 1. The last fuel bundle at the outlet end is supported by a latch (a shield plug or a side stoppers) to hold all fuel bindles at their designed positions against flow. Because of the high coolant flow rates through the fuel bundles and the acoustic pulsation of the flow provided by the primary heat pump, fuel bundles vibrate with respect to their respective equilibrium positions inside the pressure tube under reactor operating conditions [[1],[2]]. Components slide against each other and cause wear and material loss [[3]]. Material loss is a form of damage to nuclear components such as the pressure tube in the reactor core, and is therefore considered to be a major concern to the nuclear industry with regard to maintenance and safety. To determine the amount of material loss, the contact forces and sliding rates at all interfaces along with the system dynamical behaviors must be quantified with confidence at the design stage. This requires the development of a reliable and efficient dynamic model for various types of vibration of a fuel element.

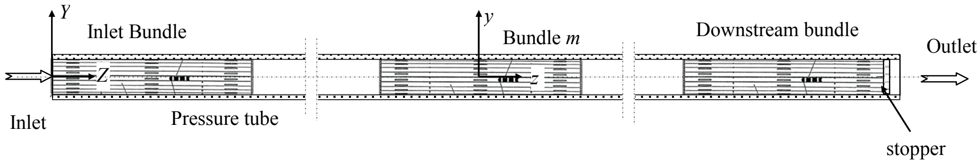

Figure 1: An overall view of a fuel channel containing a bundle string.

A fuel element consists of a thin zircaloy sheath, two zircaloy end caps, and about 30 UO_2 pellets as shown in Figure 2. During normal operations, temperatures in UO_2 pellets are high and vary significantly in the radial direction. The nominal radial gap between the sheath and pellets and axial radial gaps between the neighbouring pellets are designed to be very small. As a result, the thermal expansions of the pellets are greater than that of the sheath in the radial and axial directions. Under normal operations, fuel elements are considered as composite beams for which the classical theories of bending, axial deformation and torsion can be employed to achieve a good balance between accuracy and efficiency for static problems [[3],[4]]. In this paper, a comprehensive dynamic beam model is presented for axial, torsional, and flexural vibrations of a single fuel element.

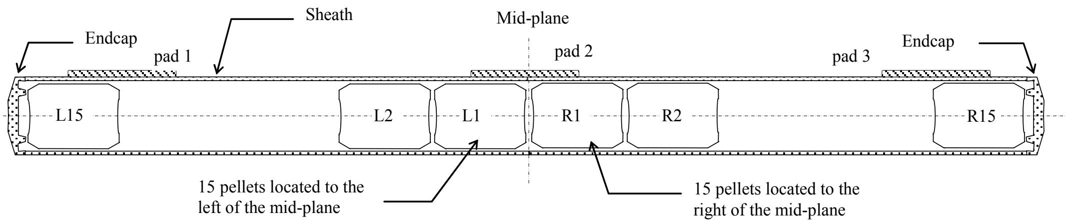

Figure 2: A sectional view of a CANDU fuel element including bearing pads

2 Equations of Motion of a Single Rod

The initial position of a fuel bundle is assumed to be concentrically placed inside a straight and undeformed pressure tube. The bundle coordinates oxyz are chosen to be originated at the initial bundle geometric centre with three axes oriented along the horizontal, vertical and axial directions, respectively, as shown in Figure 3. The coordinates (oxyz)$_i$ for fuel element i are originated at its undeformed midspan with the three axial oriented along the radial, tangential and axial directions. The bundle centre element, the element coordinates are identical to the bundle coordinates.

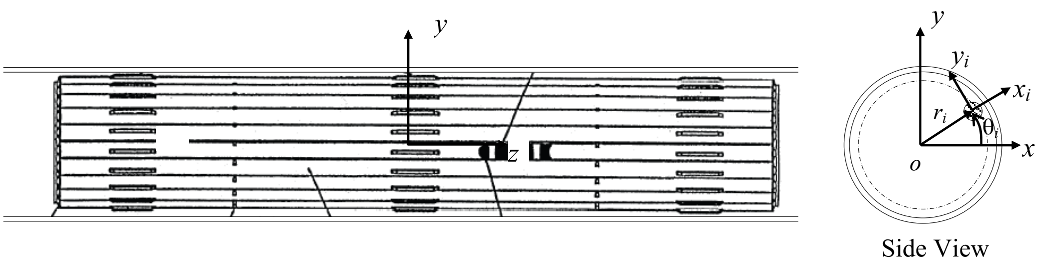

Figure 3: Coordinates used for an outer fuel element

Fuel elements are the most important constitutive components of a fuel bundle. Although the dominating dynamic response of a fuel element is bending, the axial vibration and torsional vibration cannot be ignored as they are coupled with bending vibration through the endplates. In this paper, we are concerned with the following three types of vibrational motion for a fuel rod

- lateral bending vibration in the radial and tangential directions,
- axial vibration, and
- torsional vibration.

A CANDU fuel rod has a very length-to-diameter ratio of about 38. We decided to employ the classical theories for all three types of deformations of a fuel element. The displacements of a material point in a hollow fuel sheath with appendages are related to four field variables by the following kinematic equations

$$\begin{Bmatrix} u_x \\ u_y \\ u_z \end{Bmatrix} = \underbrace{\begin{Bmatrix} 0 \\ 0 \\ w \end{Bmatrix}}_{\text{axial}} + \underbrace{\begin{Bmatrix} u \\ v \\ -\dfrac{\partial u}{\partial z}x - \dfrac{\partial v}{\partial z}y \end{Bmatrix}}_{\text{bending}} + \underbrace{\begin{Bmatrix} -\phi y \\ \phi x \\ 0 \end{Bmatrix}}_{\text{torsion}} \tag{1}$$

where $u_x, u_y,$ and u_z are the three displacements of a material point (x, y, z) in the three coordinate directions, respectively; u and v are the lateral displacements associated with bending; w is the axial displacement; ϕ is the angle of twist associated with torsion.

For convenience, the kinematic relation in Equation (1) is rewritten as

$$\begin{aligned} u_x &= u - \phi y \\ u_y &= v + \phi x \\ u_z &= w - \frac{\partial u}{\partial z}x - \frac{\partial v}{\partial z}y \end{aligned} \tag{2}$$

The above kinematic relations permit the following three non-zero strains

$$\varepsilon_{zz} = \frac{\partial w}{\partial z} - \frac{\partial^2 u}{\partial z^2} x - \frac{\partial^2 v}{\partial z^2} y, \gamma_{xz} = -\frac{\partial \varphi}{\partial z} y, \gamma_{yz} = \frac{\partial \varphi}{\partial z} x \tag{3}$$

To relate the three corresponding non-trivial stresses to the above three non-zero strains, we use the following reduced relations from the Hooke's law

$$\varepsilon_{zz} = \frac{\sigma_{zz}}{E}, \gamma_{xz} = \frac{\sigma_{xz}}{G}, \gamma_{yz} = \frac{\sigma_{yz}}{G} \tag{4}$$

where E is the modulus of elasticity; G is the shear modulus.

The strain energy of the rod for axial, flexural and torsional deformations may be written in terms of the four field variables as

$$\begin{aligned} U &= \frac{1}{2}\int_V \left\{ E\varepsilon_{zz}^2 + G\gamma_{xz}^2 + G\gamma_{yz}^2 \right\} dV \\ &= \frac{1}{2}\int_0^l \left\{ \bar{R}_{xx}\left(\frac{\partial^2 u}{\partial z^2}\right)^2 + \bar{R}_{yy}\left(\frac{\partial^2 v}{\partial z^2}\right)^2 + \bar{R}\left(\frac{\partial w}{\partial z}\right)^2 + \bar{R}_o\left(\frac{\partial \phi}{\partial z}\right)^2 + 2\bar{R}_{xy}\frac{\partial^2 u}{\partial z^2}\frac{\partial^2 v}{\partial z^2} \right. \\ &\qquad \left. - 2\bar{R}_x \frac{\partial^2 u}{\partial z^2}\frac{\partial w}{\partial z} - 2\bar{R}_y \frac{\partial^2 v}{\partial z^2}\frac{\partial w}{\partial z} \right\} dz \end{aligned} \tag{5}$$

where the seven rigidity parameters are

$$\bar{R} = \int_A E dA, \bar{R}_x = \int_A Ex dA, \bar{R}_y = \int_A Ey dA, \bar{R}_{xx} = \int_A Ex^2 dA, \bar{R}_{yy} = \int_A Ey^2 dA, \bar{R}_{xy} = \int_A Exy dA,$$
$$\bar{R}_o = \int_A G\left(x^2 + y^2\right) dA$$

The kinetic energy of the rod is written in terms of the four field variables as

$$\begin{aligned} T &= \frac{1}{2}\int_V \rho \left\{ \dot{u}_x^2 + \dot{u}_y^2 + \dot{u}_z^2 \right\} dV \\ &= \frac{1}{2}\int_0^l \left\{ \left[\bar{\rho}\dot{u}^2 + \bar{\rho}_{xx}\left(\frac{\partial \dot{u}}{\partial z}\right)^2 + \bar{\rho}\dot{v}^2 + \bar{\rho}_{yy}\left(\frac{\partial \dot{v}}{\partial z}\right)^2 + \bar{\rho}\dot{w}^2 + \bar{\rho}_o\dot{\phi}^2 \right] \right. \\ &\qquad \left. + 2\bar{\rho}_{xy}\frac{\partial \dot{u}}{\partial z}\frac{\partial \dot{v}}{\partial z} - 2\bar{\rho}_x \frac{\partial \dot{u}}{\partial z}\dot{w} - 2\bar{\rho}_y \frac{\partial \dot{v}}{\partial z}\dot{w} - 2\bar{\rho}_y \dot{u}\dot{\phi} + 2\bar{\rho}_x \dot{v}\dot{\phi} \right\} dz \end{aligned} \tag{6}$$

where the mass parameters

$$\bar{\rho} = \int_A \rho dA, \bar{\rho}_x = \int_A \rho x dA, \bar{\rho}_y = \int_A \rho y dA, \bar{\rho}_{xx} = \int_A \rho x^2 dA, \bar{\rho}_{yy} = \int_A \rho y^2 dA, \bar{\rho}_{xy} = \int_A \rho xy dA,$$

$$\bar{\rho}_o = \int_A \rho \left(x^2 + y^2 \right) dA$$

To effectively deal with bending, axial and torsional vibration, we propose to use mixed three node elements. For the bending vibration, the dynamic lateral deformations within an element are a quintic shape function of local axial coordinates; for the axial and torsional vibration, the axial displacement and the angle of twist are quadratic functions of the local axial coordinate. The four field variables are related to the nodal field variables through shape functions as follows

$$\begin{aligned} u_e &= N_1(\zeta) D_1 \bar{U}_e(t) \\ v_e &= N_1(\zeta) D_1 \bar{V}_e(t) \\ w_e &= N_2(\zeta) D_2 \bar{W}_e(t) \\ \phi_e &= N_2(\zeta) D_2 \bar{\Phi}_e(t) \end{aligned} \qquad (7)$$

where

$$N_1 = \begin{bmatrix} 1 & \zeta & \zeta^2 & \zeta^3 & \zeta^4 & \zeta^5 \end{bmatrix}, \quad N_2 = \begin{bmatrix} 1 & \zeta & \zeta^2 \end{bmatrix}.$$

$$D_1 = \begin{bmatrix} 1 & 0 & 0 & 0 & 0 & 0 \\ 0 & 1 & 0 & 0 & 0 & 0 \\ \frac{-23}{l_e^2} & \frac{-6}{l_e} & \frac{16}{l_e^2} & \frac{-8}{l_e} & \frac{7}{l_e^2} & \frac{-1}{l_e} \\ \frac{66}{l_e^3} & \frac{13}{l_e^2} & \frac{-32}{l_e^3} & \frac{32}{l_e^2} & \frac{-34}{l_e^3} & \frac{5}{l_e^2} \\ \frac{-68}{l_e^4} & \frac{-12}{l_e^3} & \frac{16}{l_e^4} & \frac{-40}{l_e^3} & \frac{52}{l_e^4} & \frac{-8}{l_e^3} \\ \frac{24}{l_e^5} & \frac{4}{l_e^4} & 0 & \frac{16}{l_e^4} & \frac{-24}{l_e^5} & \frac{4}{l_e^4} \end{bmatrix}, \quad D_2 = \begin{bmatrix} 1 & 0 & 0 \\ \frac{-3}{l_e} & \frac{4}{l_e} & \frac{-1}{l_e} \\ \frac{13}{l_e^2} & -\frac{4}{l_e^2} & \frac{2}{l_e^2} \end{bmatrix}$$

$$\bar{U}_e = \begin{Bmatrix} \begin{pmatrix} u \\ u_{,z} \end{pmatrix}_1 \\ \begin{pmatrix} u \\ u_{,z} \end{pmatrix}_2 \\ \begin{pmatrix} u \\ u_{,z} \end{pmatrix}_3 \end{Bmatrix}_e, \quad \bar{V}_e = \begin{Bmatrix} \begin{pmatrix} v \\ v_{,z} \end{pmatrix}_1 \\ \begin{pmatrix} v \\ v_{,z} \end{pmatrix}_2 \\ \begin{pmatrix} v \\ v_{,z} \end{pmatrix}_3 \end{Bmatrix}_e, \bar{W}_e = \begin{Bmatrix} w_1 \\ w_2 \\ w_3 \end{Bmatrix}_e, \bar{\Phi}_e = \begin{Bmatrix} \phi_1 \\ \phi_2 \\ \phi_3 \end{Bmatrix}_e$$

The local coordinate, ζ, is defined as $z = z_{1,e} + \zeta$. Here $z_{1,e}$ is the axial coordinate of the first node of element *e*. If N_e elements are used in a finite element model, the total kinetic and potential energies of the rod may be written as

$$T = \sum_{e=1}^{Ne} T_e, \quad U = \sum_{e=1}^{Ne} U_e \tag{8}$$

The element kinetic and potential energies are

$$T_e = \frac{1}{2}\{\dot{\bar{q}}\}_e^T [M]_e \{\dot{\bar{q}}\}_e \,.\; U_e = \frac{1}{2}\{\bar{q}\}_e^T [K]_e \{\bar{q}\}_e \tag{9}$$

where the element displacement vector, $\{q\}_e$, and the element mass matrix, $[M]_e$, and the element stiffness matrix are defined as

$$\{q\}_e = \begin{Bmatrix} \bar{U}_e \\ \bar{V}_e \\ \bar{W}_e \\ \bar{\Phi}_e \end{Bmatrix},\ [M]_e = \begin{bmatrix} \mathbf{m}_{uu} & \mathbf{m}_{uv} & \mathbf{m}_{uw} & \mathbf{m}_{u\phi} \\ & \mathbf{m}_{vv} & \mathbf{m}_{vw} & \mathbf{m}_{v\phi} \\ & & \mathbf{m}_{ww} & \mathbf{0} \\ \text{sym} & & & \mathbf{m}_{\phi\phi} \end{bmatrix}, [K]_e = \begin{bmatrix} \mathbf{k}_{uu} & \mathbf{k}_{uv} & \mathbf{k}_{uw} & \mathbf{0} \\ & \mathbf{k}_{vv} & \mathbf{k}_{vw} & \mathbf{0} \\ & & \mathbf{k}_{ww} & \mathbf{0} \\ \text{sym} & & & \mathbf{k}_{\phi\phi} \end{bmatrix}$$

All sub-matrices in the element mass and stiffness matrices are determined from

$$\mathbf{m}_{uu} = D_1^T \int_0^{le} \bar{\rho} N_1^T N_1 d\zeta D_1 + D_1^T \int_0^{le} \bar{\rho}_{xx} N_1^{'T} N_1^{'} d\zeta D_1,\ \mathbf{m}_{uv} = D_1^T \int_0^{le} \bar{\rho}_{xy} N_1^{'T} N_1^{'} d\zeta D_1,$$

$$\mathbf{m}_{uw} = -D_1^T \int_0^{le} \bar{\rho}_x N_1^T N_2 d\zeta D_2,\ \mathbf{m}_{u\phi} = -D_1^T \int_0^{le} \bar{\rho}_y N_1^T N_2 d\zeta D_2,$$

$$\mathbf{m}_{vv} = D_1^T \int_0^{le} \bar{\rho} N_1^T N_1 d\zeta D_1 + D_1^T \int_0^{le} \bar{\rho}_{yy} N_1^{'T} N_1^{'} d\zeta D_1,\ \mathbf{m}_{vw} = -D_1^T \int_0^{le} \bar{\rho}_y N_1^T N_2 d\zeta D_2$$

$$\mathbf{m}_{v\phi} = D_1^T \int_0^{le} \bar{\rho}_x N_1^T N_2 d\zeta D_2,\ \mathbf{m}_{ww} = D_2^T \int_0^{le} \bar{\rho} N_2^T N_2 d\zeta D_2,\ \mathbf{m}_{\phi\phi} = D_2^T \int_0^{le} \bar{\rho}_o N_2^T N_2 d\zeta D_2$$

$$\mathbf{k}_{uu} = D_1^T \int_0^{le} \bar{R}_{xx} N_1^{''T} N_1^{''} d\zeta D_1, \mathbf{k}_{uv} = D_1^T \int_0^{le} \bar{R}_{xy} N_1^{''T} N_1^{''} d\zeta D_1,\ \mathbf{k}_{uw} = -D_1^T \int_0^{le} \bar{R}_x N_1^{''T} N_2^{'} d\zeta D_2,$$

$$\mathbf{k}_{vv} = D_1^T \int_0^{le} \bar{R}_{yy} N_1^{''T} N_1^{''} d\zeta D_1,\ \mathbf{k}_{vw} = -D_1^T \int_0^{le} \bar{R}_y N_1^{''T} N_2^{'} d\zeta D_2, \mathbf{k}_{ww} = D_2^T \int_0^{le} \bar{R} N_2^{'T} N_2^{'} d\zeta D_2,$$

$$\mathbf{k}_{\phi\phi} = D_2^T \int_0^{le} \bar{R}_o N_2^{'T} N_2^{'} d\zeta D_2$$

The following equations of motion may be obtained using the Lagrange equations

$$[M]\{\ddot{q}\}+[K]\{q\}=\{0\} \tag{10}$$

where $\{q\}$ is the global displacement vector; $[M]$ and $[K]$ are global mass and stiffness matrices.

The elimination approach is employed to deal with the homogeneous boundary conditions imposed on the two ends of the rod.

3 Numerical Results

A straight hollow tube (495.3 mm in length, 11.5 mm in outer diameter, and 10.8 mm in inner diameter) with three bearing pads is used to simulate an outer fuel element of an advanced CANDU fuel bundle. The material properties of un-irradiated zircaloy are determined at an operating temperature of 300 C. Values of the material properties concerning vibration are density of 7850 kg/m^3, modulus of elasticity of 77.2 GPa, Poisson's ratio of 0.37, and shear modulus of 28.175 GPa. The tube has three identical bearing pads at three axial locations (44.5 mm, 247.65 mm, 450.85 mm, respectively, from the upstream end). Each pad is 25.4 mm in length (the axial dimension), 2.5 mm in width (the circumferential dimension), and 1.45 mm in thickness (the radial dimension). In is test cases, the boundary conditions are free at the upstream and clamped at the downstream.

For a tube without pads, there is no coupling among the bending vibration in the bundle radial (or *x*-) direction, bending vibration in the bundle tangential or (*y*-) direction, the axial vibration and the torsional vibration. Each natural frequency corresponds to a pure mode of deformation. However, for a fuel element with bearing pads, as shown in Figure 4, whose geometric centre is located at the bundle radial line, the *x*- and *y*- axes are principal axes. The following geo-mass and geo-stiffness parameters vanish: $\overline{\rho}_y$, $\overline{\rho}_{xy}$ $\overline{R}_y$, and $\overline{R}_{xy}$. Consequently, only the bending vibration in the *x*-direction is coupled with the axial vibration through the mass and stiffness matrices; and the bending in the y-direction is coupled with the torsional vibration through the mass matrix.

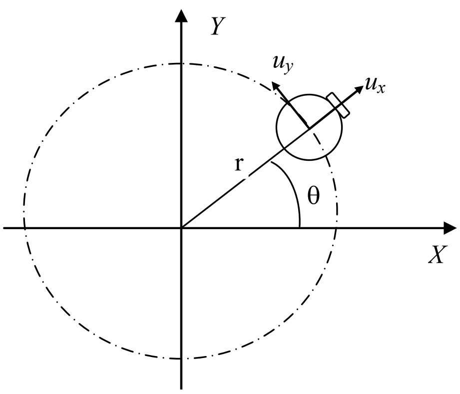

Figure 4: Lateral displacements of a rod in space-fixed and body-fixed coordinate systems

To model the effects of appendages, the tube is first divided into a number of uniform segments. Each segment is meshed using the mixed three node beam elements. The system equations of motion are obtained by direct assembly of segment equations of motion. A convergence study concluded that a total of 38 beam elements is sufficient to achieve satisfactory accuracy for the first 20 modes of vibration of a cantilever tube with and without appendages. Table 1 gives the first 20 natural frequencies of the rod with and without the appendages along with the dominating deformation associated with each frequency. Mode coupling due to the presence of appendages is seen clearly in Figure 5 for mode 10. In addition to mode coupling, it is interesting to note that the stiffening effects of appendages is maintained in the bending vibration in the radial direction. However, the softening effects of appendages prevail in the bending vibration in the tangential direction.

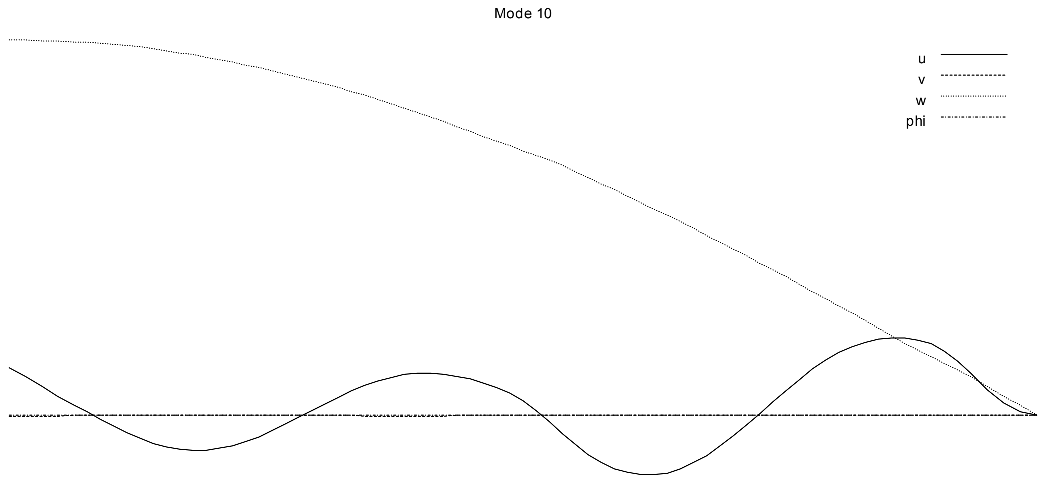

Figure 5: Coupling of bending and axial vibration due to bearing pads

4 Conclusions

This paper presents a mixed beam finite element scheme for free axial, flexural and torsional vibration of a CANDU fuel element without pellets. Numerical results obtained for an outer fuel element consisting of fuel sheath with and without bearing pads as appendages show that the effects of appendages on the natural frequencies and mode shapes are significant. The dynamic model of a fuel element is being implemented into a computer code for predicting flow induced vibration in CANDU fuel string subjected to large scale dynamic contact.

Modes	without appendages		with appendages	
	Frequencies	Deformation	Frequencies	Dominating Deformation
1	30.858	1st Bending in *x* or *y*	30.089	1st Bending in *y*
2	30.858	1st Bending in *y* or *x*	31.157	1st Bending in *x*
3	193.215	2nd Bending in *x* or *y*	188.632	2nd Bending in y
4	193.215	2nd Bending in *y* or *x*	195.103	2nd Bending in *x*
5	540.241	3rd Bending in *x* or *y*	537.952	3rd Bending in *y*
6	540.241	3rd Bending in *y* or *x*	540.972	3rd Bending in *x*
7	1046.052	1st torsion	1038.077	1st torsion
8	1056.473	4th Bending in *x* or *y*	1038.232	4th Bending in *y*
9	1056.473	4th Bending in *y* or *x*	1064.523	4th Bending in *x*
10	1731.524	1st axial	1712.292	1st axial
11	1741.767	5th Bending in *x* or *y*	1726.504	5th Bending in *y*
12	1741.767	5th Bending in *y* or *x*	1746.639	5th Bending in x
13	2593.404	6th Bending in *x* or *y*	2525.487	6th Bending in *y*
14	2593.404	6th Bending in *y* or *x*	2636.258	6th Bending in *x*
15	3138.156	2nd torsion	3110.095	2nd torsion
16	3608.247	7th Bending in *x* or *y*	3533.657	7th Bending in *y*
17	3608.247	7th Bending in *y* or *x*	3649.286	7th Bending in *x*
18	4782.641	8th Bending in *x* or *y*	4625.054	8th Bending in *y*
19	4782.641	8th Bending in *y* or *x*	4883.433	8th Bending in *x*
20	5194.572	2nd Axial	5155.905	2nd Axial

Table 1 Natural frequencies (Hz) of a cantilever hollow tube

Acknowledgement

The authors would like to thank Dr. Dezi Yang of CANDU Energy Inc. for his technical advice and support. The financial support from NSERC and SNC Lavalin Nuclear through a collaborative research grant is gratefully acknowledged.

References

[1] Paidoussis, M.P. 1982. “A review of flow-induced vibrations in reactors and reactor components, Nuclear Engineering and Design, v 74, n 1, p 31-60, 1982.

[2] Pettigrew, M.J. 1993. The vibration behavior of nuclear fuel under reactor conditions. Nuclear Science and Engineering, 114(3), 179-189

[3] M. Yetisir and N. L. Fisher. 1997. “Prediction of pressure tube fretting-wear damage due to fuel vibration,” Nuclear Engineering and Design, v 176, n 3, p 261-271.

[4] J. Veeder, and M. H. Schankula, 1974. Bowing of Pelletized Fuel Elements: Theory and In-Reactor Experiments. Nuclear Engineering and Design 29, 164-179.

[5] Tayal, M., 1989. Modelling the bending/bowing of composite beams such as nuclear fuel: the BOW code. Nuclear Engineering and Design 116, 149-159.